Bioelectrochemistry 86 (2012) 60–66

Contents lists available at SciVerse ScienceDirect

Bioelectrochemistry

journal homepage: www.elsevier.com/locate/bioelechem

Direct electrochemistry and electrocatalysis of hemoglobin immobilized on polyacrylamide-P123 film modified glassy carbon electrode

Jinxia Li, Jing Tang, Lihui Zhou *, Xia Han , Honglai Liu

Key Laboratory for Advanced Materials and Department of Chemistry, East China University of Science and Technology, Shanghai 200237, China

ARTICLE INFO

Article history:
Received 23 May 2011
Received in revised form 3 February 2012
Accepted 4 February 2012
Available online 18 February 2012

Keywords:
Direct electron transfer
Hemoglobin
Polyacrylamide
P123

ABSTRACT

A novel organic mesoporous material, polyacrylamide-P123 (PAM-P123) composite film, was used to incorporate hemoglobin (Hb) onto the surface of glassy carbon (GC) electrode for studying the direct electron transfer of Hb and fabricating a sensitive biosensor of H_2O_2. Compared with inorganic mesoporous material, the PAM-P123 composite film has better film-forming property, which is particularly useful for preparing modified electrodes on various substrates for voltammetric measurements. The cyclic voltammetry of Nafion/Hb/PAM-P123/GC modified electrode showed a couple of well-defined and quasi-reversible redox peaks at about 0.317 V (vs. SCE) in pH 7.0 phosphate buffer solution. The Nafion/Hb/PAM-P123/GC modified electrode showed a fast amperometric response and good stability for the detection of hydrogen peroxide. The results indicate that the PAM-P123 film has a promising potential in fabricating third-generation electrochemical biosensors.

1. Introduction

Electrochemical sensors were widely applied in real clinical, environment, food and industry related samples due to their high sensitivity and selectivity, fast response, low cost, and potential for continuous online detection of complex systems [1–4]. Since the catalytic process and chemical properties of redox enzymes with mediator are very complex, utilization of the direct electrochemistry of redox enzymes has attracted much interest in recent years. However, it is difficult for an enzyme or a protein to carry out a direct electrochemical reaction due to several factors. Firstly, the electroactive centers of redox proteins are deeply embedded in the insulated protein shells, resulting in a very long distance between the electroactive centers and underlying electrodes, so it is difficult to transfer electrons directly to the conventional electrodes [5]. Secondly, loss of electrochemical activities and bioactivities often occur when proteins are adsorbed on the electrode surface [6]. An effective method to realize direct electrochemistry of enzymes is to incorporate them into cast films modified on electrode surface [7,8]. Great efforts have been devoted to explore new supporting materials and suitable methods of immobilization of proteins onto the electrode surface to obtain their direct electrochemical reactions. Various materials such as surfactants [9–11], polymers [12–15] and nanomaterials [16–25] have been exploited for immobilizing proteins and facilitating the electron transfer of proteins.

The inorganic mesoporous materials have been widely applied in the study of direct electron transfer of proteins, due to their unique properties of high surface area, good biocompatibility and nontoxicity [26–28]. The mesoporous materials can provide favorable microenvironments for proteins and enhanced electron transfer between the electroactive centers of proteins and electrodes surface. However, the electronic insulating property of inorganic silica mesoporous materials and the relatively weak adhesive stability between mesoporous materials and electrode surface inhibit their application in the electrochemical field [29]. An assembly of stable sensing structures requires strong binding of supporting materials to solid supports [12]. Thus, we expect to use a kind of organic mesoporous material, which not only inherits the advantages of their polymer matrix but also presents large surface area, as a new film-forming material to study the direct electron transfer of redox protein. To the best of our knowledge, no electrochemistry of heme proteins in organic mesoporous modified electrode has been studied.

In our previous work, a novel organic mesoporous material polyacrylamide-P123 (PAM-P123) composite film was prepared using a simple water-evaporation-induced self-assembly method, which has lamellar structure and good film-forming property [30]. In this paper, the PAM-P123 composite film was used for immobilizing Hb on glassy carbon (GC) electrode surface and studying the electron transfer of Hb. The structural features of Hb immobilized on PAM-P123 film were characterized using UV–Vis spectra and AFM method. The effect of PAM-P123 composite film on direct electron transfer of Hb was investigated by cyclic voltammetry (CV) method. The influences of scan rate and pH value of buffer solution on Nafion/Hb/PAM-P123/GC were investigated in detail. The electrocatalitic reduction of hydrogen peroxide on Nafion/Hb/PAM-P123/GC modified electrode was also studied.

* Corresponding author at: Department of Chemistry, East China University of Science and Technology, 130 Meilong Road, Shanghai 200237, China. Tel.: +86 21 64253235.
E-mail address: lhzhou@ecust.edu.cn (L. Zhou).

1567-5394/$ – see front matter © 2012 Elsevier B.V. All rights reserved.
doi:10.1016/j.bioelechem.2012.02.002

2. Experimental

2.1. Reagents

Hb (MW 64,500, from bovine blood) was purchased from Sigma Co. Ltd. (USA). Pluronic P123 ($EO_{20}PO_{70}EO_{20}$, MW = 5800) was obtained from BASF. Acrylamide (AM), ammonium persulfate (APS) and formaldehyde (37–40 wt.%) were obtained from Shanghai Lin-Feng Chemical Reagent Ltd. (China). Phenol was purchased from Shanghai Fei-Da Trade Ltd. Phosphate buffer solutions (PBS) containing 0.1 mol·l^{-1} KCl (pH 7.0) were prepared by mixing stock standard solutions of Na_2HPO_4 (0.1 mol·l^{-1}) and KH_2PO_4 (0.1 mol·l^{-1}). All solutions were prepared with doubly distilled water.

2.2. Synthesis of PAM-P123 composite film

The synthesis of PAM-P123 composite was performed according to the reference [30] with some modifications. Firstly, a soluble low-molecular-weight PAM precursor (p-PAM) was prepared by a basic polymerization method. AM (1.0 g) was dissolved in 80 ml H_2O at room temperature in a three-necked flask equipped with a reflux condenser and a magnetic stirrer. The solution was deoxygenated with bubbled nitrogen at 60 °C for 15 min. Then 20 ml of APS (1.4×10^{-1} mol·l^{-1}) initiator aqueous solution was added into the flask, after 60 min, a p-PAM sol was obtained.

The above PAM precursor, p-PAM, was mixed with 30 ml P123 aqueous solution (1.03×10^{-2} mol·l^{-1}) and stirred at 40 °C for 4 h. Phenol (0.13 g) and formaldehyde (0.34 g) were dissolved in 50 ml water, and this solution was used as a cross-linking reagent. After the cross-linking reagent was added, the solution was heated to 70 °C and stirred for 60 min under nitrogen atmosphere. The PAM-P123 solution was obtained.

Finally, the obtained PAM-P123 solution was dialyzed against doubly distilled water for several times to remove AM monomer, phenol and formaldehyde using a semi-permeable membrane.

2.3. Electrode modification

Prior to preparation of modified electrode, GC electrode of 3.0 mm in diameter was mechanically polished to a mirror finish with 0.05 μm alumina slurry, then ultrasonically washed with 1:1 HNO_3 (v/v), NaOH (1.0 mol·l^{-1}), ethanol and redistilled water for 30 s, respectively. In a typical procedure, 10 μl of the PAM-P123 solution was dropped on the pretreated GC surface and dried for 2 h at room temperature. Then 10 μl of 10 mg·ml^{-1} Hb solution was spread onto the dry PAM-P123 film surface. Until the Hb/PAM-P123 film dried for about 3 h, 5 μl of Nafion solution was dropped and dried for 1 h at room temperature. The modified electrodes were noted as Nafion/Hb/PAM-P123/GC. The electrodes were stored at 4 °C in a refrigerator.

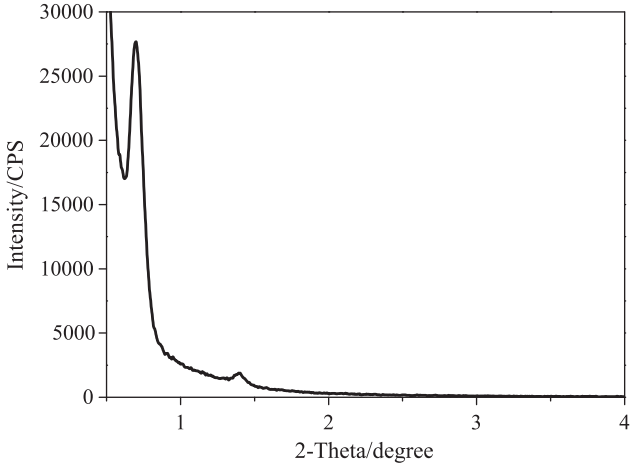

Fig. 1. Low-angle XRD patterns of PAM-P123.

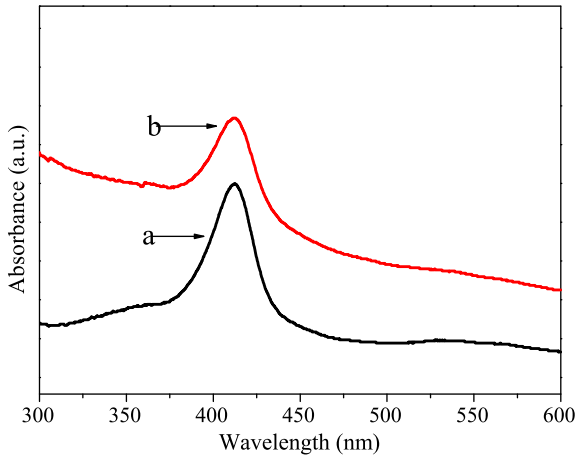

Fig. 2. UV–Vis spectra of (a) Hb and (b) Hb/PAM-P123 in 0.1 M PBS (pH 7.0).

2.4. Apparatus and measurements

Electrochemical experiments were carried out on a CHI 430A electrochemical workstation (Shanghai Chenhua, China) with a three-electrode system: a modified GC electrode as the working electrode, a platinum electrode as counter electrode and a saturated calomel electrode (SCE) as reference electrode. The CV experiments were carried out in 5 ml of 0.1 mol·l^{-1} PBS (pH 7.0) at room temperature. The solutions were bubbled with highly purified nitrogen for at least 20 min to remove oxygen, and nitrogen atmosphere were maintained over the solutions during the experiments.

The low-angle X-ray powder diffraction (XRD) patterns were recorded using a Rigaku D/max 2550 VB/PC diffractometer with the Cu Kα radiation (λ = 0.154056 nm). UV–Vis spectra were recorded on Shimadzu UV-2450 spectrophotometer. The AFM topography images were obtained in tapping mode by an AFM (AJ-III, Aijian Nanotechnology Inc., China) with a triangular microfabricated cantilever (Mikro Masch Co., Russia).

3. Results and discussion

3.1. Characterization of PAM-P123 by XRD

Fig. 1 shows the low-angle XRD pattern obtained from the PAM-P123 solution deposited on glass substrate. The XRD diffraction peaks of PAM-P123 film appeared at 0.70° and 1.40° indexing as the (100) and (200) planes, which suggests a typical feature of lamellar structure [31,32]. The PAM-P123 composite film with lamellar structure can be easily formed on solid surface, which is suitable for immobilization of protein and modification of electrode.

3.2. UV–Vis spectra

It is important to immobilize Hb on the surface of the modified electrode without its denaturation. It is well known that the position of the Soret absorption band of Hb in UV–Vis spectra can provide information about possible denaturation of Hb. Fig. 2 exhibits the UV–Vis spectra of Hb and Hb/PAM-P123 on quartz glass substrate. Hb/PAM-P123 film gives a Soret band at 412 nm, which is the same as the Soret band at 412 nm for Hb film. These results indicate that the secondary structure of Hb immobilized on the surface of PAM-

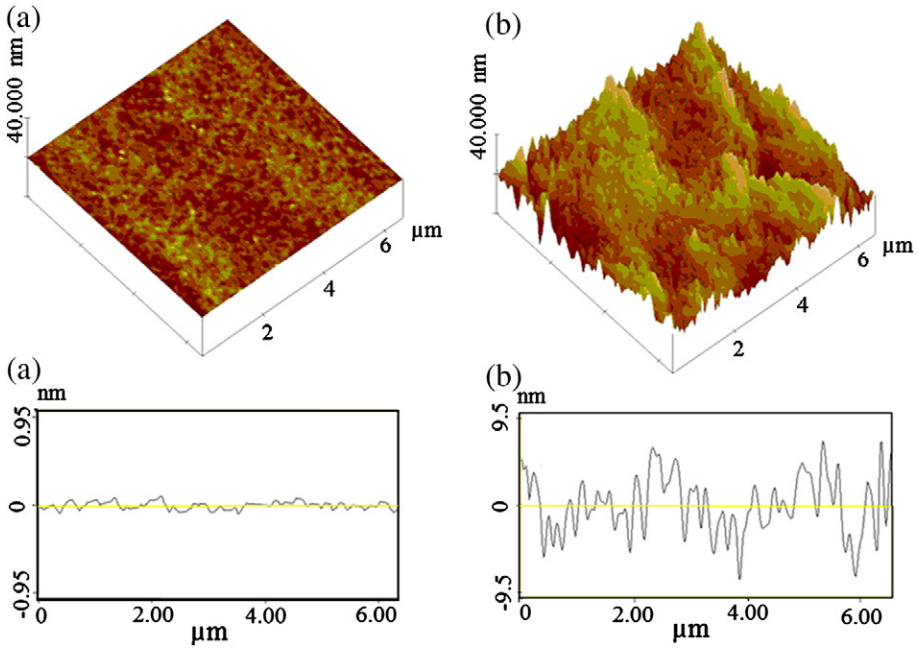

Fig. 3. AFM images and corresponding profile analysis of (a) PAM-P123 and (b) Hb/PAM-P123 film.

P123 is not destroyed. Thus, the PAM-P123 composite film can be used to immobilize Hb molecules while retaining their native structures and biological activities.

3.3. AFM and SEM

The structural features of Hb immobilized on PAM-P123 film were characterized using AFM method. Fig. 3 shows the surface morphologies of PAM-P123 film and Hb/PAM-P123 film on surfaces of mica wafer and the corresponding profile analyses, respectively. A relatively smooth surface can be clearly seen in AFM image of PAM-P123 film (Fig. 3a), which indicates that the PAM-P123 solution can be uniformly distributed to be a homogeneous film when it is dried on a smooth surface. After the casting of the Hb solution on the PAM-P123 film, the surface of Hb/PAM-P123 film (Fig. 3b) becomes much rougher with many bright convex spots resembling small mountains, and the profile analysis exhibits large fluctuations different from that of the virgin PAM-P123 film. Comparatively, the root-mean-square roughnesses of the two figures were 0.13 and 3.74 nm, respectively. It has been suggested that the Hb protein is loaded on the smooth PAM-P123 film to be aggregates [33]. The thickness of PAM-P123 was measured using AFM height image of PAM-P123 with scratching method [34]. Fig. 4 shows AFM images and corresponding profile analysis of PAM-P123 film. The film thickness of PAM-P123 can be estimated to be 280 ± 30 nm from the cross-sectional analysis.

SEM was also used to characterize and compare the morphologies of PAM-P123 and Hb/PAM-P123 with the results shown in Fig. 5. It can be seen that the PAM-P123 film is fairly smooth on a large area (Fig. 5a). The image in Fig. 5b shows that the aggregates of the immobilized Hb molecules are distributed regularly, resulting in a film-like structure. The SEM results are consistent with the AFM results (Fig. 3).

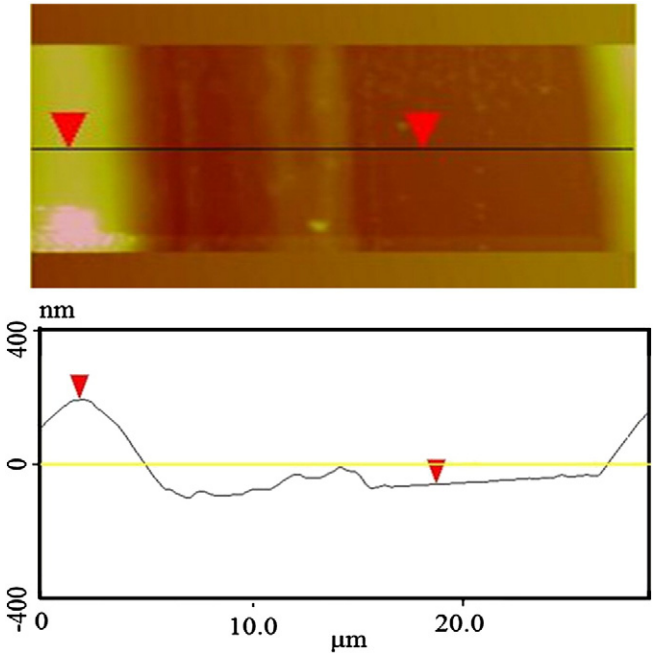

Fig. 4. AFM images and corresponding profile analysis of PAM-P123 film.

3.4. Direct electrochemistry of Nafion/Hb/PAM-P123/GC modified electrode

As mentioned above, the PAM-P123 film was prepared using a water-evaporation-induced self-assembly method. The film with a biomembrane-like lamellar structure can be formed on glass substrate or metal electrode surface, which can be used as interface layer to immobilize biological components. Therefore, the PAM-P123 film was used for immobilizing Hb on GC electrode surface and studying the electron transfer of Hb in the following electrochemistry experiment.

The PAM-P123 film can be considered as a hybrid material, which retains the original properties of PAM and P123 while giving to the composite distinct chemical and physical properties that differ from those exhibited by the individual components. PAM has a long hydrophobic carbon backbone with hydrophilic amide groups. P123 is an amphiphilic triblock copolymer that consists of hydrophilic PEO segments and hydrophobic PPO segments. The interaction between PAM-P123 and Hb is complicated, mainly containing hydrophobic interaction, hydrogen bond and van der Waals force [35]. In this way, PAM-P123 film can adsorb Hb on its surface. Since PAM-P123 film and Hb are water soluble to some extent, Nafion was used to enhance

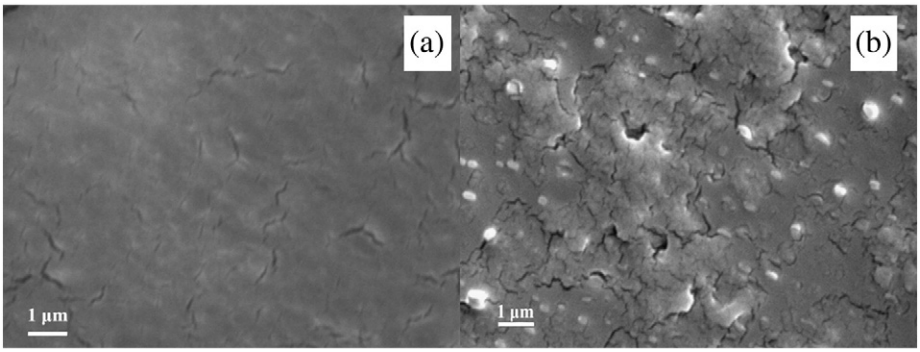

Fig. 5. SEM micrographs of (a) P123-PAM and (b) Hb/PAM-P123.

stability of the modified electrode and to prevent Hb molecules release of under the conditions of liquid phase and electricity.

The electrochemistry properties of Nafion/Hb/PAM-P123/GC modified electrode were characterized by the CV method. Fig. 6 shows the CVs at 0.3 $V \cdot s^{-1}$ in pH 7.0 PBS of PAM-P123/GC electrode and Nafion/Hb/PAM-P123/GC electrode. No clear peak was observed in the CV of PAM-P123/GC electrode (Fig. 6a), indicated that PAM-P123 film is electroinactive in potential window. A couple of well-defined and quasi-reversible redox peaks can be observed at Hb/PAM-P123/GC electrode (Fig. 6b). Under the same conditions, a more obvious couple of well-defined and reversible redox peaks can be observed in the CV of Nafion/Hb/PAM-P123/GC electrode at about −0.366 V and −0.268 V (Fig. 6c), which can be ascribed to the redox of the electroactive center Fe(III)/Fe(II) of Hb. Besides, the formal potential [$E^{\circ\prime} = (E_{pa} + E_{pc})/2$] is −0.317 V (vs. SCE), which is more positive than the values of Hb in inorganic mesoporous material modified electrode (e.g., $E^{\circ\prime}$ of Hb/SBA-15/GC is −0.343 V (vs. SCE) and $E^{\circ\prime}$ of Hb/MCF/GC is −0.358 V(vs. SCE) [36]. This may be attributed to a specific influence of film environment on $E^{\circ\prime}$ of heme proteins that had been reported previously [37]. Based on the above experiments results, it can be concluded that the main reason for the dramatic improved electrochemical properties of Nafion/Hb/PAM-P123/GC is that PAM-P123 film provides a favorable biomembrane-like microenvironment to avoid denaturation of Hb molecules and facilitate transfer electrons directly with underlying electrodes [38,39].

The effect of scan rate on the electrochemical response of Nafion/Hb/PAM-P123/GC is demonstrated in Fig. 7a. The reduction and oxidation peak currents for Hb increase linearly with the scan rate from 0.1 to 1.0 $V \cdot s^{-1}$ (Fig. 7b). The regression equations are $I_{pc}/A = 3.65(\pm 0.03) \times 10^{-6} v/V \cdot s^{-1} - 1.91(\pm 1.86) \times 10^{-8}$ and $I_{pa}/A = -3.41(\pm 0.04) \times 10^{-6} v/V \cdot s^{-1} - 1.88(\pm 2.52) \times 10^{-8}$ with correlation coefficients of 0.9997 and 0.9994, respectively. On the contrary, charge (Q) values calculated by integration of the oxidation peaks are independent of the scan rates in the same range. These results correspond to the characteristics of surface or thin layer electrochemistry [40–42], suggesting that the electroactive HbFe (III) in the film are converted to HbFe (II) on the forward scan and vice versa. The surface concentration of electroactive Hb (Γ^*) was estimated from the integration of the oxidation peak in the CVs according to the

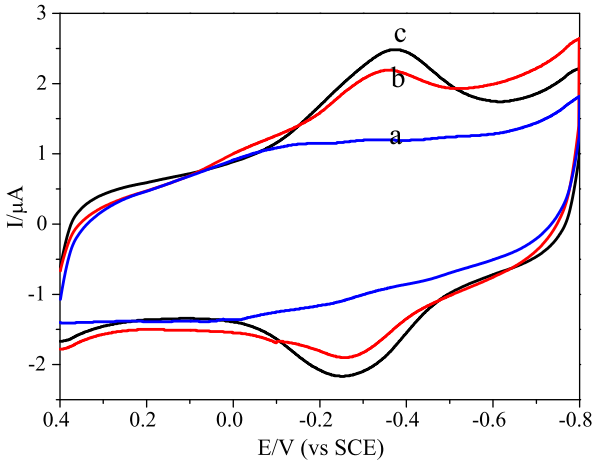

Fig. 6. CVs of (a) PAM-P123/GC electrode, (b) Hb/PAM-P123/GC, and (c) Nafion/Hb/PAM-P123/GC electrode at 0.3 $V \cdot s^{-1}$ in pH 7.0 PBS.

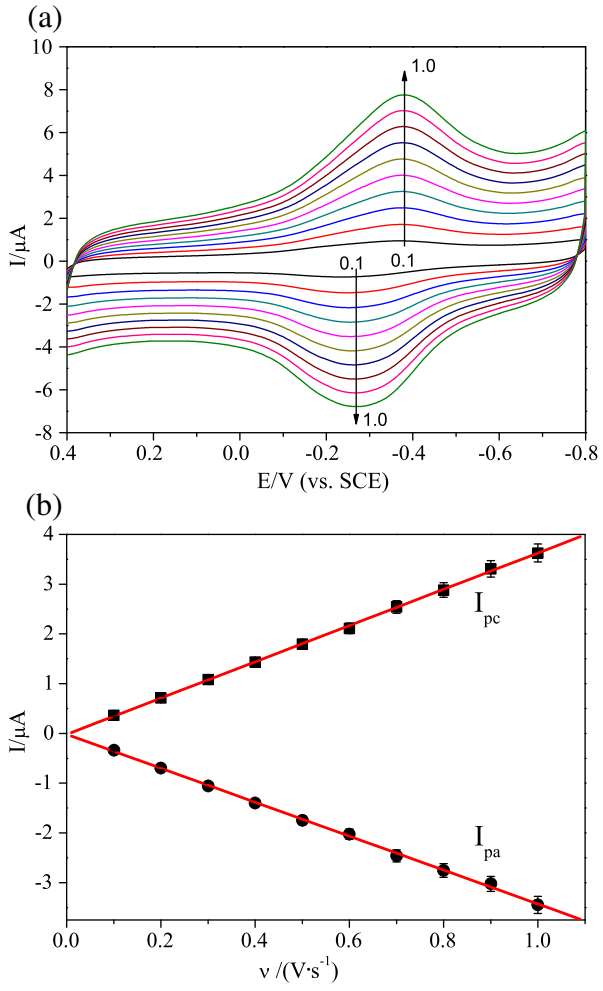

Fig. 7. (a) CVs of Nafion/Hb/PAM-P123/GC electrode in pH 7.0 PBS at different scan rates. From inner to outside: 0.1–1.0 $V \cdot s^{-1}$.(b) Redox peak current/μA as a function of the scan rate/$V \cdot s^{-1}$.

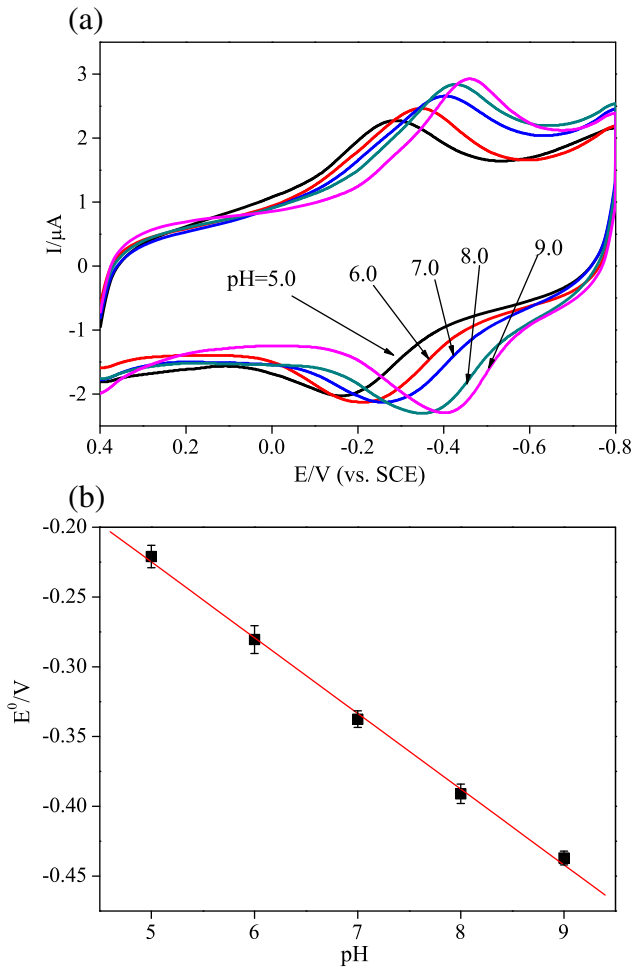

Fig. 8. (a) CVs of Nafion/Hb/PAM-P123/GC electrode at 0.3 $V \cdot s^{-1}$ in PBS with different pH values.(b) Dependence of the formal potential on the solution pH.

equation:

$$\Gamma* = Q(nFA)^{-1} \quad (1)$$

wherein Q is the charge involved in the reaction ($Q = 5.20 \times 10^{-7}$ C), n is the number of electrons transferred ($n = 1$), F is the Faraday's constant(F = 96500 C/mol), and A is the electrode area

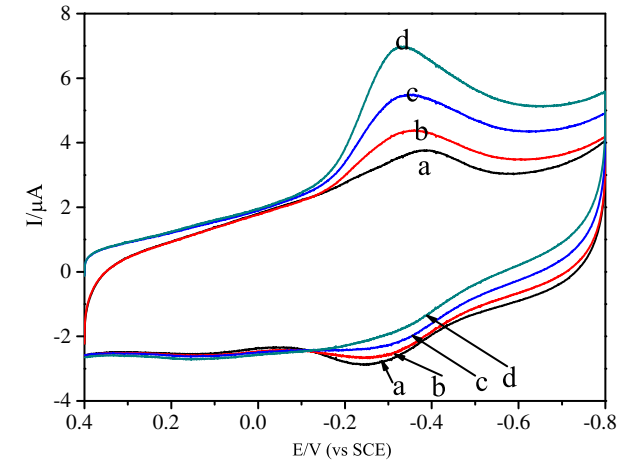

Fig. 9. CVs of Nafion/Hb/PAM-P123/GCE electrode in PBS solution (pH 7.0) containing different H_2O_2 concentrations: (a) 0, (b) 5, (c) 10, (d) 15 $\mu mol \cdot l^{-1}$.

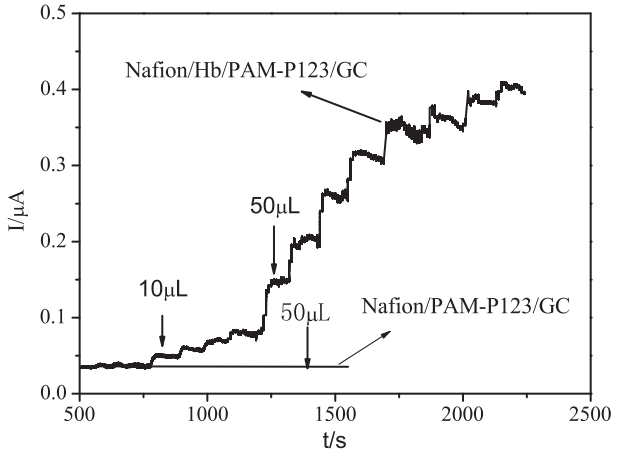

Fig. 10. Amperometric response of Nafion/Hb/PAM-P123/GC at −0.4 V upon successive additions of H_2O_2 in PBS (pH 7.0).

($A = 7.06 \times 10^{-2}$ cm^2). Based on the above equation, Γ^* can be calculated to be 7.64×10^{-11} $mol \cdot cm^{-2}$. This value is only 0.35% of the total amount of Hb deposited on the electrode surface. The relative amount of the electroactive proteins on the electrode surface are always below 1% for all the heme proteins. These results indicate that only those proteins in the inner layers of the films close to the electrode and with a suitable orientation can exchange electrons with the electrode surface. The Γ^* value obtained in our experiment is about three times larger than that of theoretical monolayer coverage of Hb (1.89×10^{-11} $mol \cdot cm^{-2}$) [43]. This may suggest that a multilayer of Hb participate in the electron transfer process on the PAM-P123 modified electrode.

The effect of pH value of the supporting electrolyte on the peak potentials of the Nafion/Hb/PAM-P123/GC electrode was also investigated. As seen from Fig. 8a, an increase in the solution pH value caused a negative shift in both cathodic and anodic peak potentials. The formal potential ($E^{\circ\prime}$) [$E^{\circ\prime} = (E_{pa} + E_{pc})/2$] with a strong dependence on the pH value of the external solutions indicated that the transfer of one proton and one electron per heme group occurred according to the reaction shown below [44]. Fig. 8b shows a linear relationship between $E^{\circ\prime}$ and pH value with the slope of 54 mV/pH, which is close to the theoretically expected value (59 mV/pH) for one electron and one proton reaction [45].

$$\text{Hb hemeFe (III)} + H^+ + e^- \rightleftharpoons \text{Hb hemeFe (II)} \quad (2)$$

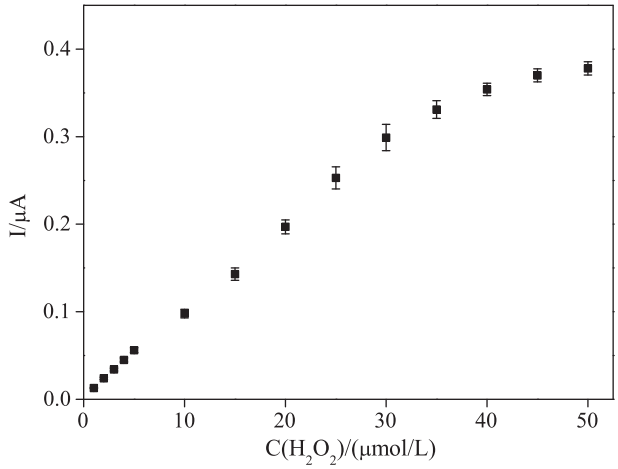

Fig. 11. Calibration curves of steady-state currents versus concentrations of H_2O_2 for Nafion/Hb/PAM-P123/GC electrodes.

Table 1
Linear range and detection limit for different H_2O_2 biosensors based on the direct electron transfer of Hb.

Different H_2O_2 biosensors	Immobilized Hb technique description	Linear range (mol l^{-})	Detection limit (mol l^{-})	Reference
Hb/P123-NGP/GC	nanotechnology	1.0×10^{-5}–1.5×10^{-4}	8.24×10^{-6}	[46]
Hb/SDS/TiO_2/GC	liquid phase deposition technique	5.0×10^{-7}–4.0×10^{-5}	8.7×10^{-8}	[47]
Hb/IL/CILE	carbon ionic liquid electrode method	1.0×10^{-4}–5.0×10^{-3}	4×10^{-5}	[48]
Hb/sol–gel/CPE	sol–gel technology	5×10^{-6}–7×10^{-4}	–	[24]
Hb/PAM-P123/GC	water-evaporation-induced self-assembly method	1.0×10^{-6}–3.0×10^{-5}	4×10^{-7}	This work

3.5. Electrocatalytic properties of Nafion/Hb/PAM-P123/GC electrodes

The electrocatalytic properties of Nafion/Hb/PAM-P123/GC modified electrodes for the reduction of H_2O_2 were investigated. Fig. 9 shows the cyclic voltammograms of the electrode in 0.1 M PBS (pH 7.0) in absence or presence of H_2O_2. When H_2O_2 (5 μmol·l^{-1}) is present in PBS, the anodic peak current of Nafion/Hb/PM-P123/GC electrode decreases and the cathodic peak current increases (Fig. 9b). Increasing the H_2O_2 concentration, the cathodic peak currents continue to increase, while the anodic peak currents disappear gradually (Fig. 9c and d). These results indicate that the Hb immobilized in PAM-P123 film on GC has electrocatalytic activity to the reduction of H_2O_2.

Fig. 10 shows the amperometric response of modified electrodes at −0.4 V upon successive additions of 5×10^{-4} mol·l^{-1} H_2O_2 in PBS. The amperometric response reaches 95% of the steady-state current in less than 5 s on the Nafion/Hb/PAM-P123/GC modified electrode, showing a very fast electrocatalytic response. In addition, with increasing added concentration of H_2O_2, the response of the Nafion/Hb/PAM-P123/GC modified electrode increased. For comparison, no obvious electrocatalytic response of H_2O_2 was observed on the Nafion/PAM-P123/GC modified electrode without Hb incorporated. These results suggest that the catalytic reduction reaction was due to the interaction between immobilized Hb and H_2O_2.

Calibration curves of steady-state currents versus concentrations of H_2O_2 for Nafion/Hb/PAM-P123/GC electrodes were shown in Fig. 11. The reduction peak current increased with increasing concentration of H_2O_2. Under optimal conditions, the linear response range of the sensor to H_2O_2 concentration was from 1 to 30 μM with a correlation coefficient of 0.9990. The calculated detection limit was 4×10^{-7} mol·l^{-1} (S/N = 3). When the concentration of H_2O_2 was higher than 30 μmol·l^{-1}, a plateau was observed, showing a characteristic of the Michaelis–Menten kinetic mechanism. Table 1 shows the performance of the here proposed H_2O_2 biosensor in comparison with some previous works [46–48,24]. As can be seen, the results obtained with Hb/PAM-P123/GC electrode present a reasonable linear range and a detection limit lower than that of some works reported in the literature.

The apparent Michaelis–Menten constant (K_m), which reflects both the enzymatic affinity, can be calculated from the electrochemical version of the Lineweaver–Burk equation [49]:

$$1/I_{ss} = 1/I_{ss,max} + K_m/I_{ss,max}C \quad (3)$$

wherein I_{ss} is the steady-state current after the addition of substrate, C is the bulk concentration of the substrate, and $I_{ss,max}$ is the maximum current measured under saturated substrate conditions. In this system, its linear regression equation is $y = 76.35(\pm1.41)x + 2.11(\pm0.54)$ ($R = 0.9986$, $n = 10$), wherein y and x stand for $1/I_{ss}$ ($(\mu A)^{-1}$) and $1/C$ ($(\mu M)^{-1}$), respectively. From the intercept and slope of this linear regression equation, K_m was calculated to be 0.036 mmol·l^{-1} for the Nafion/Hb/PAM-P123/GC modified electrode. This value is smaller than Hb/3-mercaptopropylphosphonic acid/Au electrode of 0.042 mM [50], K_m of 0.176 mM for Hb-CuO NWB/GC electrode [20], K_m of 0.51 mM for Hb/P123/PG electrode [39], 0.898 mM Hb in silica sol–gel film [51]. The small K_m value indicates that the immobilized Hb on the Nafion/Hb/PAM-P123/GC electrode has a high biological affinity for H_2O_2 and higher catalytic activity for reduction of H_2O_2.

The stability of the Nafion/Hb/PAM-P123/GC modified electrode was investigated. After the modified electrode was stored at 4 °C in refrigerator for about 7 days, the sensor retained about 95% of its initial sensitivity for the reduction of H_2O_2, while a month later, 90% efficiency was retained. On the other hand, the experiments on six electrodes that were made independently showed an acceptable reproducibility with the relative standard deviations of 5.3% for the current determinations of 10 μmol·l^{-1} H_2O_2.

4. Conclusions

In this work, direct electrochemistry of Hb was observed when the proteins were immobilized on organic mesoporous material PAM-P123 composite film. The electrode reactions showed a surface-controlled process at the scan rate range from 0.1 to 1.0 V·s^{-1}. The apparent standard potentials of Hb on the PAM-P123 film change linearly with solution pH in the range from 5.0 to 9.0, with a slope of 54 mV/pH. These results suggest that PAM-P123 composite film provides an efficient strategy and a new promising platform for the study of electron transfer of redox proteins. Good electrocatalytic properties of the Nafion/Hb/PAM-P123/GC electrode toward hydrogen peroxide indicate that the films have a promising potential in fabricating the third-generation electrochemical biosensors.

Acknowledgement

This work was supported by the National Natural Science Foundation of China (Project No. 21176065), the Fundamental Research Funds for the Central Universities and the 111 Project of China (No. B08021).

References

[1] G. Dryhurst, K.M. Kadish, F. Scheller, R. Rennerberg, Biological electrochemistry, , Academic Press, New York, 1982.
2 E. Bakker, Electrochemical sensors, Anal. Chem. 76 (2004) 3285–3298.
3 I. Willner, B. Willner, E. Katz, Biomolecule–nanoparticle hybrid systems for bioelectronic applications, Bioelectrochemistry 70 (2007) 2–11.
4 D. Du, X. Xu, S. Wang, A. Zhang, Reagentless amperometric carbohydrate antigen 19–9 immunosensor based on direct electrochemistry of immobilized horseradish peroxidase, Talanta 71 (2007) 1257–1262.
5 L. Liu, F. Zhao, L. Liu, J. Li, B. Zeng, Improved direct electron transfer and elec trocatalytic activity of horseradish peroxidase immobilized on gemini surfactant–polyvinyl alcohol composite film, Colloids Surf., B. 68 (2009) 93–97.
6 J.F. Rusling, Enzyme bioelectrochemistry in cast biomembrane-like films, Acc. Chem. Res. 31 (1998) 363–369.
7 P. He, N. Hu, J.F. Rusling, Driving forces for layer-by-layer self-assembly of films of SiO_2 nanoparticles and heme proteins, Langmuir 20 (2004) 722–729.
8 M.J.A. Shoddiky, A.A.J. Torriero, T. Sagara, N. Nakashima, J.F. Rusling, Electrochemical properties of myoglobin embedded in Langmuir–Blodgett and cast films of synthetic lipids, Biosens. Bioelectron. 26 (2011) 1775–1787.
9 F. Wang, X.C. Chen, Y.X. Xu, S.S. Hu, Z.N. Gao, Enhanced electron transfer for hemoglobin entrapped in a cationic gemini surfactant films on electrode and the fabrication of nitric oxide biosensor, Biosens. Bioelectron. 23 (2007) 176–182.
10 Z. Lu, Q. Huang, J. Rusling, Films of hemoglobin and didodecyldimethylammonium bromide with enhanced electron transfer rates, J. Electroanal. Chem. 423 (1997) 59–66.
11 X.J. Han, W.M. Huang, J.B. Jia, Direct electrochemistry of hemoglobin in egg-phosphatidylcholine films and its catalysis to H_2O_2, Biosens. Bioelectron. 17 (2002) 741–746.
12 U. Lange, N.V. Roznyatovskaya1, V.M. Mirsky, Conducting polymers in chemical sensors and arrays, Anal. Chim. Acta 614 (2008) 1–26.
13 L.M. Moretto, P. Bertoncello, F. Vezzà, P. Ugo, Electrochemistry of cytochrome c incorporated in Langmuir-Blodgett films of Nafion® and Eastman AQ 55®, Bioelectrochem 66 (2005) 29–34.

14 P. Ugo, N. Pepe, L.M. Moretto, M. Battagliarin, Direct voltammetry of cytochrome c at trace concentrations with nanoelectrodes ensembles, J. Electroanal. Chem. 560 (2003) 51–58.
15 K. Lin, Y. Yu, S. Chen, Direct electrochemistry of hemeproteins at organic modified electrodes: an electrochemical biosensor for determination of hydrogen peroxide using nanocomposite of poly(methylene blue) and FAD hybrid film, Sens. Actuators B: Chem. 157 (2011) 202–210.
16 Q. Feng, K. Liu, J. Fu, Y. Zhang, Z. Zheng, C. Wang, Y. Du, W. Ye, Direct electrochemistry of hemoglobin based on nano-composite film of gold nanopaticles and poly (diallyldimethylammonium chloride) functionalized grapheme, Electrochim. Acta 60 (2012) 304–308.
17 D. Cao, N. Hu, Direct electron transfer between hemoglobin and pyrolytic graphite electrodes enhanced by Fe_3O_4 nanoparticles in their layer-by-layer self-assembly films, Biophys. Chem. 121 (2006) 209–217.
18 D. Nie, Y. Liang, T. Zhou, X. Li, G. Shi, L. Jin, Electrochemistry and electrocatalytic of hemoglobin immobilized on FDU-15-Pt mesoporous materials, Bioelectrochem. 79 (2010) 248–253.
19 M. Miyahara, A. Vinu, K.Z. Hossain, T. Nakanishi, K. Ariga, Adsorption study of heme proteins on SBA-15 mesoporous silica with pore-filling models, Thin Solid Films 499 (2006) 13–18.
20 Y.M. Li, Q. Zhang, J.H. Li, Direct electrochemistry of hemoglobin immobilized in CuO nanowire bundles, Talanta 83 (2010) 162–166.
21 H.Y. Gu, A.M. Yu, H.Y. Chen, Direct electron transfer and characterization of hemoglobin immobilized on a Au colloid-cysteamine-modified gold electrode, J. Electroanal. Chem. 516 (2001) 119–126.
22 Z.H. Dai, S.Q. Liu, H.X. Ju, Direct electron transfer and enzymatic activity of hemoglobin in a hexagonal mesoporous silica matrix, Biosens. Bioelectron. 19 (2004) 861–867.
23 L.W. Du, H. Jiang, X.H. Liu, E.K. Wang, Biosynthesis of gold nanoparticles assisted by *Escherichia coli* DH5α and its application on direct electrochemistry of hemoglobin, Electrochem. Commun. 9 (2007) 1165–1170.
24 Q.L. Wang, G.X. Lu, B.J. Yang, Direct electrochemistry and electrocatalysis of hemoglobin immobilized on carbon paste electrode by silica sol–gel film, Biosens. Bioelectron. 19 (2004) 1269–1275.
25 X.J. Han, W.L. Cheng, Z.L. Zhang, Direct electron transfer between hemoglobin and a glassy carbon electrode facilitated by lipid-protected gold nanoparticles, BB A-Bioenergetics. 1556 (2002) 273–277.
26 A. Walcarius, Electrochemical applications of silica-based organic–inorganic hybrid materials, Chem. Mater. 13 (2001) 3351–3372.
27 H.H.P. Yiu, P.A. Wright, Enzymes supported on ordered mesoporous solids: a special case of an inorganic–organic hybrid, J. Mater. Chem. 15 (2005) 3690–3700.
28 Z. Dai, S. Liu, H. Ju, H. Chen, Direct electron transfer and enzymatic activity of hemoglobin in a hexagonal mesoporous silica matrix, Biosens. Bioelectron. 19 (2004) 861–867.
29 A. Walcarius, Impact of mesoporous silica-based materials on electrochemistry and feedback fromelectrochemical science to the characterization of these ordered materials, C.R. Chimie. 8 (2005) 693–712.
30 J. Tang, Y. Fan, J. Hu, H. Liu, Fabrication of ordered lamellar polyacrylamide/P123 composite membranes via solvent-evaporation-induced self-assembly, J. Colloid Interface Sci. 331 (2009) 191–195.
31 X. Yu, Z. Xu, S. Han, H. Che, X. Yan, A. Liu, Synthesis of well-ordered lamellar mesoporous molybdenum oxide, Colloids Surf. A Physicochem. Eng. Asp. 333 (2009) 194–198.
32 H. Zhang, Z. Jin, X. Wang, A new synthesis of lamellar-mesostructured silica by using poly(ethylene glycol) distearate as template, Mater. Res. Bull 43 (2008) 2979–2985.
33 Y. Hu, H. Sun, N. Hu, Assembly of layer-by-layer films of electroactive hemoglobin and surfactant didodecyldimethylammonium bromide, J. Colloid Interface Sci. 314 (2007) 131–140.
34 Hu. Han Xia, Liu Honglai Jun, Hu. Ying, SEBS aggregate patterning at surface studied by atomic force microscopy, Langmuir 22 (2006) 3428–3433.
35 L. Shen, R. Huang, N.F. Hu, Myoglobin in polyacrylamide hydrogel films: direct electrochemistry and electrochemical catalysis, Talanta 56 (2002) 1131–1139.
36 J.X. Li, Z.Y. Xiong, L.H. Zhou, X. Han, J. Hu, H.L. Liu, Effects of pore structure of mesoporous silicas on the electrochemical properties of hemoglobin, Microporous Mesoporous Mater. 130 (2010) 333–337.
37 Y. Xu, C. Hu, S. Hu, Direct electron-transfer of native hemoglobin in blood: Kinetics and catalysis, Bioelectrochemistry 72 (2008) 135–140.
38 H. Sun, N. Hu, H. Ma, Direct electrochemistry of hemoglobin in polyacrylamide hydrogel films on pyrolytic graphite electrodes, Electroanalysis 12 (2000) 1064–1070.
39 N. Jia, Q. Lian, Z. Wang, H. Shen, A hydrogen peroxide biosensor based on direct electrochemistry of hemoglobin incorporated in PEO–PPO–PEO triblock copolymer film, Sens. Actuators B: Chem. 137 (2009) 230–234.
40 A.J. Bard, L.R. Faulkner, Electrochemical methods—fundamentals and applications, second ed. Wiley, New York, 2001.
41 C. Shi, Fred C. Anson, Simple electrochemical procedure for measuring the rates of electron transfer across liquid/liquid interfaces formed by coating graphite electrodes with thin layers of nitrobenzene, J. Phys. Chem. B 102 (1998) 9850–9854.
42 T. Chung, Fred C. Anson, Catalysis of the electroreduction of O_2 by cobalt 5,10,15,20-tetraphenylporphyrin dissolved in thin layers of benzonitrile on graphite electrodes, J. Electroanal. Chem. 508 (2001) 115–122.
43 S.F. Wang, T. Chen, Z.L. Zhang, X.C. Shen, Z.X. Lu, D.W. Pang, K.Y. Wong, Direct electrochemistry and electrocatalysis of heme proteins entrapped in agarose hydrogel films in room-temperature ionic liquids, Langmuir 21 (2005) 9260–9266.
44 E. Trushina, R. Oda, J. Landers, C. Mcmurray, Determination of nitrite and nitrate reduction by capillary ion electrophoresis, Electrophoresis 18 (1997) 1890–1898.
45 A.M. Bond, Modern polarographic methods in analytical chemistry, Marcel Dekker, New York, 1980 27–45.
46 X.X. Xu, J.X. Zhang, F. Guo, W. Zheng, H.M. Zhou, B.L. Wang, Y.F. Zheng, Y.B. Wang, Y. Cheng, X. Lou, B.Z. Jang, A novel amperometric hydrogen peroxide biosensor based on immobilized Hb in Pluronic P123-nanographene platelets composite, Colloids Surf., B 84 (2011) 427–432.
47 R. Wang, J. dong Zhang, Y. Hu, Liquid phase deposition of hemoglobin/SDS/TiO_2 hybrid film preserving photoelectrochemical activity, Bioelectrochem. 81 (2011) 34–38.
48 A. Safavi, N. Maleki, O. Moradlou, M. Sorouri, Direct electrochemistry of hemoglobin and its electrocatalytic effect based on its direct immobilization on carbon ionic liquid electrode, Electrochem. Commun. 10 (2008) 420–423.
49 W.Z. Jia, K. Wang, Z.J. Zhu, H.T. Song, X.H. Xia, One-step immobilization of glucose oxidase in a silica matrix on a Pt electrode by an electrochemically induced sol–gel process, Langmuir 23 (2007) 11896–11900.
50 Y. Chen, B. Jin, L. Guo, X. Yang, W. Chen, G. Gu, L. Zheng, X. Xia, Hemoglobin on phosphonic acid terminated self-assembled monolayers at a gold electrode: immobilization, direct electrochemistry, and electrocatalysis, Chem. Eur. J. 14 (2008) 10727–10734.
51 Q.L. Wang, G.X. Lu, B.J. Yang, Hydrogen peroxide biosensor based on direct electrochemistry of hemoglobin immobilized on carbon paste electrode by a silica sol–gel film, Sens. Actuator, B 99 (2004) 50–57.